

Chapter 6

Decomposition of Oxalate in Dilute Aqueous Solutions:
Evidence for the Strong Synergism of Ozonolysis
Combined with Ultrasonic Irradiation

Abstract

The simultaneous application of ultrasonic irradiation with ozonation was demonstrated to be effective for the oxidation of oxalic acid ($\text{H}_2\text{C}_2\text{O}_4/\text{HC}_2\text{O}_4^-/\text{C}_2\text{O}_4^{2-}$), a particularly recalcitrant pollutant, to CO_2 and H_2O . Degradation rates obtained using sonolytic ozonation were found to be more than 16-times faster than predicted by the linear addition of the independent systems. Model calculations and batch ozone decomposition experiments in the presence of oxalate and/or ultrasound suggest that ozone efficiently reacts with carboxyl anion radical, CO_2^- produced by the OH-radical attack on HC_2O_4^- . We propose that this reaction propagates a free-radical chain mechanism which increases OH-radicals concentrations within the bulk solution. We believe that this mechanism is responsible for the rapid degradation of oxalate, perhaps magnified by the additional $\cdot\text{OH}$ -radicals that results from the thermal decomposition of O_3 within acoustic cavitation bubbles. Oxalate was also oxidized by the mixture of H_2O_2 and O_3 . However, addition of H_2O_2 to systems undergoing sonolytic ozonation did not appreciably affect the observed degradation kinetics, indicating that the $\text{O}_3/\text{ultrasound}/\text{HC}_2\text{O}_4^-$ system is predominantly driven by free-radical chemistry.

Introduction

Oxalic acid is a common phytochemical that is also produced during incomplete biomass burning,¹ during the photodegradation of humic substances and natural organic matter (NOM)^{2,3}, and via the ring-opening oxidation of aromatic compounds⁴⁻⁹. As a consequence, oxalate [$\text{oxalate} \equiv \text{H}_2\text{C}_2\text{O}_4$ (oxalic acid) + HC_2O_4^- (bioxalate) + $\text{C}_2\text{O}_4^{2-}$ (oxalate)] is routinely detected in terrestrial and aquatic environments as well as in atmospheric aerosols.^{1,2,10} Oxalate is relatively recalcitrant towards oxidation and accumulates in natural waters where it can lead to unrestrained microbial growth.^{2,11,12} Exposure to high oxalate concentrations has detrimental health effects such as kidney and renal cell damage, nutrient deficiencies, and lithiasis.¹³⁻¹⁶ Therefore, any tertiary wastewater process should include provisions for complete degradation of oxalates.

The chemistry of aqueous oxalate degradation has been investigated for more than 50 years. Attempts to chemically decompose oxalate include treatment with various transition metals^{17,18}, permanganate¹⁹, peroxydisulfate²⁰, bromine²¹, and with metal-oxide photocatalysts.²² More recently, several studies have focused on the use of several metal-ion catalysts with ozonolysis to enhance the degradation of oxalate in aqueous solution.²³⁻²⁷ Oxalic acid is quite resistant to oxidation with ozonolysis alone; however in the presence of these metal catalysts the complete degradation and mineralization of oxalate in aqueous solution to CO_2 is observed. The increased oxidation of the modified ozone system seems to proceed through a mechanism whereby ozone recycles high oxidation states of metal ions, which in turn oxidize chelated oxalate.^{24,26}

While $\text{H}_2\text{C}_2\text{O}_4$, HC_2O_4^- , and $\text{C}_2\text{O}_4^{2-}$ are known scavengers of e^-_{aq} and $\cdot\text{OH}$,²⁸⁻³⁰ previous investigations have indicated that $\cdot\text{OH}$ -mediated degradation of oxalate by high-

frequency ultrasound results in minimal degradation.^{31,32} In an attempt to improve the efficiency of the sonolytic degradation of oxalate, we examined the combination of ultrasonic irradiation with ozonolysis. Using the coupled techniques, we found that oxalate degradation rates significantly exceeded the addition of their independent rates. While previous investigations have also found the combination of ozone and ultrasonic irradiation to be effective at enhancing the degradation and mineralization of various organic solutes in aqueous solution,^{6,33-35} the synergism observed in our system appears to be unique.

The principal objective of this study is to investigate the mechanism of the strong synergistic effect of sonolysis combined with ozonolysis for the oxidation of oxalic acid. The degradation pathways of the individual oxidation techniques are discussed and several degradation mechanisms are considered which may account for the observed rate enhancements when the two systems are combined.

Experimental Section

Experiments were performed in a 605 mL bench-scale sonochemical reactor (Allied Signal-ELAC Nautik USW). The ELAC reactor employs a bottom-mounted 358 kHz transducer operated between 0 and 100 Watts. The reactor is a glass vessel with an integrated water jacket for cooling. Aqueous samples were chilled to 15 °C with a 1.5 kW thermostat (VWR 1157). The vessel is sealed with a hemispherical glass top with several sampling ports. One of the ports was left open to the atmosphere to allow for gas exchange. The emitting area of the ELAC transducer is 23.6 cm². The reported applied power for the small reactors has been previously determined using standard calorimetric procedures.³⁶

Ozone was generated with a corona discharge ozone generator (Orec V10-0). The O₂ feed gas was dried and purified with a molecular sieve and drierite cartridge (Alltech) prior to entering the instrument. The O₂/O₃ mixture was delivered to a solution in the reactor via a medium porosity glass frit and was sparged during sonication. Varying the voltage and flow rates of the of the ozone generator regulated ozone concentrations. Gas flow rates were monitored with a gas flow meter (Gilmont Instruments). Steady state concentrations of ozone in the small reactor ranged from 0 to 400 μM.

Analytical methods and equipment

Aliquots were sampled with a glass syringe that was fitted with a stainless steel needle and were stored in amber glass vials and then analyzed to quantify the concentration of the substrates. Anion concentrations were quantified using a Dionex Bio LC ion chromatograph. Separations were carried out on a 25 cm AS11 column with

a 0.01 – 0.1 M NaOH eluent with a flow rate of 2 mL/min. Total organic carbon concentrations were measured with a Shimadzu TOC 5000 A organic carbon analyzer with a Shimadzu ASI 5000A autosampler. A heated course catalyst bed was heated to 680 °C . Samples were acidified with HCl to pH 1-2 and purged for 1 minute prior to injection with instrument grade air to remove any dissolved carbonate or bicarbonate. Samples were measured in triplicate.

Aqueous ozone concentrations were determined in a 1 cm pathlength quartz cuvette with a Hewlett Packard 8452 A diode-array spectrophotometer at $\lambda = 260$ nm ($\epsilon_{\text{aq O}_3} = 3292 \text{ M}^{-1}\text{cm}^{-1}$). Ozone concentrations were monitored indirectly with iodometry in solutions containing oxalate due to absorption interferences at 260 nm. Sample aliquots were added to flasks containing KI (1% w/w, 0.06M) in a phosphate solution at pH 7, and the absorbance of I_3^- ($\text{I}^- + \text{I}_2 \rightarrow \text{I}_3^-$) was monitored at $\lambda = 350$ nm and a set of calibrations were performed to demonstrate the direct correlation with ozone concentrations.

H_2O_2 solutions were prepared by dilution of 30% H_2O_2 (EM Science) in purified H_2O . Concentrations were quantified by UV-spectroscopy at $\lambda = 248$ nm ($\epsilon_{\text{H}_2\text{O}_2} = 25 \text{ M}^{-1}\text{cm}^{-1}$), or by iodometry using ammonium molybdate (0.02% w/w, 1.1 mM) as a catalyst.³⁷ pH measurements were made with a Beckman Altex 71 pH meter, and a Beckman glass pH electrode (model 39843).

Oxalate degradation kinetics were determined under constant levels of ozonolysis and ultrasonic irradiation. The O_3 steady-state concentrations for these experiments were determined before the addition of $\text{H}_2\text{C}_2\text{O}_4$ or the imposition of the acoustic field. In order to ensure that $[\text{O}_3]_{\text{ss}}$ remained constant during the course of an experiment, a separate

vessel containing ultrapure H₂O was sparged with the same ozone stream and the [O₃] was determined. The maximum variation in [O₃]_{ss} during the experiment was ± 10 μM.

Separate experiments were performed to investigate the decomposition kinetics of ozone in the presence of ultrasound and/or oxalate. Ultra-pure water was sparged with O₂/O₃ for an hour until [O₃]_{aq} reached ~ 100 μM. To initiate a reaction, oxalate solutions were added into the O₃ solution. At this point, flow of O₂/O₃ gas supply was interrupted, and [O₃] at t = 0 was determined.

Oxalic Acid (H₂C₂O₄) (Baker, >99.5%), KI (Sigma, ≥99.0), NaH₂PO₄ (Mallinckrodt, ≥99.0), Na₂HPO₄ (Mallinckrodt, ≥99.0), NaCO₂H (Mallinckrodt, ≥99.0), NaC₂H₃O₂ (Mallinckrodt, ≥99.0), (NH₄)₆Mo₇O₂₄ • 4H₂O (Alfa Products), and H₂O₂ (EM Science, 30 %wt) were used without further purification. Water used for sample preparation was purified with a Millipore Milli-Q UV Plus system (*R* = 18.2 MΩ cm⁻¹). All pH measurements were made with a Beckman Altex 71 pH meter. The reaction kinetics were measured in un-buffered systems.

Results and Discussion

Oxalate Acid Speciation

Our experiments were performed by adding $\text{H}_2\text{C}_2\text{O}_4 \cdot 2 \text{H}_2\text{O}$ to ultrapure water. The addition of oxalic acid resulted in an average pH depression from 5 to 3. The two acid dissociation constants, $\text{pK}_{a1} = 1.2$ and $\text{pK}_{a2} = 4.2$,³⁸ suggest that all three forms of oxalate will be present in solution. The relative amounts of these species are given by

$$\alpha_{\text{H}_2\text{C}_2\text{O}_4} = \frac{[\text{H}_2\text{C}_2\text{O}_4]}{[\text{H}_2\text{C}_2\text{O}_4]_t}, \alpha_{\text{HC}_2\text{O}_4^-} = \frac{[\text{HC}_2\text{O}_4^-]}{[\text{H}_2\text{C}_2\text{O}_4]_t}, \text{ and } \alpha_{\text{C}_2\text{O}_4^{2-}} = \frac{[\text{C}_2\text{O}_4^{2-}]}{[\text{H}_2\text{C}_2\text{O}_4]_t} \quad (1a, b, c)$$

where

$$[\text{H}_2\text{C}_2\text{O}_4]_t = [\text{H}_2\text{C}_2\text{O}_4] + [\text{HC}_2\text{O}_4^-] + [\text{C}_2\text{O}_4^{2-}] \quad (2)$$

$$\alpha_{\text{H}_2\text{C}_2\text{O}_4} = \frac{[\text{H}_3\text{O}^+]^2}{[\text{H}_3\text{O}^+]^2 + K_{a1}[\text{H}_3\text{O}^+] + K_{a1}K_{a2}} \quad (3)$$

$$\alpha_{\text{HC}_2\text{O}_4^-} = \frac{K_{a1}[\text{H}_3\text{O}^+]}{[\text{H}_3\text{O}^+]^2 + K_{a1}[\text{H}_3\text{O}^+] + K_{a1}K_{a2}} \quad (4)$$

$$\alpha_{\text{C}_2\text{O}_4^{2-}} = \frac{K_{a1}K_{a2}}{[\text{H}_3\text{O}^+]^2 + K_{a1}[\text{H}_3\text{O}^+] + K_{a1}K_{a2}} \quad (5)$$

From equations 1-5 at pH 3, we estimate that 93% of the total oxalate is present as bioxalate, HC_2O_4^- , and 6% as oxalate, $\text{C}_2\text{O}_4^{2-}$.

HC_2O_4^- Degradation Kinetics in the Presence of Ultrasound, O_3 , and US/ O_3

The degradation of oxalate in aqueous solution was performed with ultrasonic irradiation and continuous ozonolysis. HC_2O_4^- was oxidized with apparent zero-order reaction kinetics as shown in Figures 1 and 2.

$$-\left(\frac{d[\text{oxalate}]}{dt}\right) = R_{-ox} = k_{-ox} \quad (6)$$

Profiles of normalized solute concentrations vs. time were fit to a normalized pseudo zero-order rate constant, k'_{-ox} .

$$\frac{[C_2H_2O_4]}{[C_2H_2O_4]_o} = 1 - \left(\frac{k_{-ox}}{[C_2H_2O_4]_o}\right)t = 1 - (k'_{-ox})t \quad (7)$$

During the course of the experiments, solutions remained clear and colorless; no additional products were observed using standard chromatographic techniques. The extent of $HC_2O_4^-$ oxidation was independently followed by monitoring the concentration of the total organic carbon (TOC) remaining in solution as $HC_2O_4^-$ was oxidized to CO_2 and H_2O according to the following stoichiometry:



TOC degradation rates, R_{TOC} , also followed zero-order degradation kinetics and were fit using a variation of equation 7. Normalized rate constants for $HC_2O_4^-$ and TOC degradation, k'_{-ox} and k'_{TOC} , respectively, for each system were essentially identical, indicating that the degradation of $HC_2O_4^-$ resulted in the mineralization of the solute to CO_2 (i.e., no free radical polymerization to produce higher molecular weight compounds).

The maximum rate of sonolytic decomposition was obtained at 358 kHz (100 W) with a normalized rate constant of $^{US}k'_{-ox} = 9.24 \times 10^{-4} \text{ min}^{-1}$ ($[H_2C_2O_4]_o = 0.9 \text{ mM}$) (Fig. 1). This represents a 50% $HC_2O_4^-$ loss after 10 hours. The rate of $HC_2O_4^-$ degradation by simple ozonolysis at a steady-state concentration of $[O_3]_{ss} = 340 \text{ } \mu\text{M}$ was slightly faster with a rate constant of $^{O_3}k'_{-ox} = 1.07 \times 10^{-3} \text{ min}^{-1}$ ($[H_2C_2O_4]_o = 0.9 \text{ mM}$, $\text{pH} = 3$) (Fig. 2). This represents a half-life of ~ 8 hours. In contrast to the minimal effects achieved with

each technique individually, the simultaneous application of ozone and ultrasound significantly enhanced the degradation of HC_2O_4^- . A maximum normalized degradation rate constant of $^{US/O_3}k'_{-ox} = 3.14 \times 10^{-2} \text{ min}^{-1}$ was obtained at 358 kHz, 100 W with $[\text{O}_3]_{ss} = 350 \mu\text{M}$. (Fig. 2) This combined system resulted in complete degradation of the sample and all organic carbon (i.e., TOC) within one hour. The synergistic action of O_3 and ultrasound enhanced oxalate degradation rates 16-fold compared to the simple linear addition of the two independent systems.

HC_2O_4^- degradation rates were measured in the sonolytic ozone system at two separate ozone concentrations, 150 μM and 350 μM , as a function of ultrasonic power density (PD) at 358 kHz. (Fig. 3) At the lower ozone concentration, a maximum rate constant of $^{US/O_3}k'_{-ox} = 9.9 \times 10^{-3} \text{ min}^{-1}$ was obtained at 83.3 W/L. Subsequent increases in power from 83 W/L to 133 and to 167 Watts did not result in further enhancements. The normalized pseudo zero-order rate constant at the higher ozone concentrations increased proportionally to the applied power density between 0 and 83 W/L as expressed in the following relationship

$$^{US/O_3}k'_{-ox} = 3.1 \times 10^{-4} [\text{PD (W L}^{-1}\text{)}] + 2.4 \times 10^{-4} \quad (9)$$

Increasing the power from 83 to 166 W/L further enhanced degradation rates, but only by 20%.

HC_2O_4^- Degradation Mechanisms

HC_2O_4^- Degradation with Ultrasonic Irradiation

The thermal decomposition of water vapor in acoustic cavitation bubbles leads to the formation of $\cdot\text{OH}$ and $\text{H}\cdot$ as shown in equation 10.



Subsequent radical reactions produce other oxidizing species such as the hydroperoxyl radical, $\text{HO}_2\cdot$ and superoxide, $\text{O}_2\cdot^-$. These radical species ultimately self-react (i.e., undergo termination) with one another to produce H_2O , O_2 , and H_2O_2 .³⁹⁻⁴³ The second-order rate constants, k_2 , as measured by pulse radiolysis³⁰, indicate that $\cdot\text{OH}$ reacts more slowly with oxalic acid as compared to either anion:

$$k_2[\cdot\text{OH} + \text{H}_2\text{C}_2\text{O}_4 (\text{HC}_2\text{O}_4^-; \text{C}_2\text{O}_4^{2-})] = 1.4 \times 10^6 (4.7 \times 10^7; 7.7 \times 10^6) \text{ M}^{-1}\text{s}^{-1} \quad (11\text{a, b, c})$$

HC_2O_4^- is not known to react with $\text{HO}_2\cdot$ or H_2O_2 , and it reacts very slowly with $\cdot\text{O}_2^-$ ($k < 0.2 \text{ M}^{-1}\text{s}^{-1}$)⁴⁴. Therefore, in the presence of ultrasound, the degradation of oxalic acid only occurs via reactions with $\cdot\text{OH}$.

$$-\left(\frac{d[\text{H}_2\text{C}_2\text{O}_4]_t}{dt}\right) \approx R_{(\cdot\text{OH}/\text{HC}_2\text{O}_4^-)} = k[\cdot\text{OH}][\text{HC}_2\text{O}_4^-] \quad (12)$$

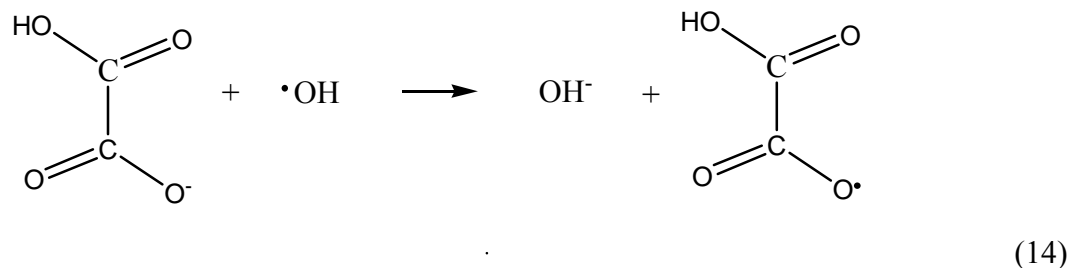
In the presence of ultrasound alone, many dilute organic species dissolved in water decay quasi-exponentially with apparent first-order dependence on the solute, suggesting steady-state concentrations for the sonically generated $\cdot\text{OH}$.^{6,45-47} However, the sonolytic degradation profile shown in Figure 1 suggests an apparent zero-order dependence on HC_2O_4^- . This indicates that the rate-limiting step in the overall reaction is the concentration of $\cdot\text{OH}$ in solution (i.e., the rate of $\cdot\text{OH}$ production via acoustic cavitation is equal to the rate of loss due to reactions with the solute and radical termination reactions). Hua and Hoffmann⁴³ previously measured the $\cdot\text{OH}$ production rate in water in a similar ultrasonic reactor operating at 513 kHz. At 39 W of applied

power, they determined an $\cdot\text{OH}$ (aq) production rate of $\sim 5 \times 10^{-9} \text{ M s}^{-1}$. This production rate is smaller than our observed degradation rate for oxalate obtained using 358 kHz at 100 W, $^{\text{US}}k_{\text{-ox}} = 1.4 \times 10^{-8} \text{ M s}^{-1}$; however, by scaling Hua and Hoffmann's rate to 100 W we can estimate that the rate of $\cdot\text{OH}$ production is equal to the rate of loss via reaction with HC_2O_4^- . Equating equations 6 and 12, and assuming steady-state conditions

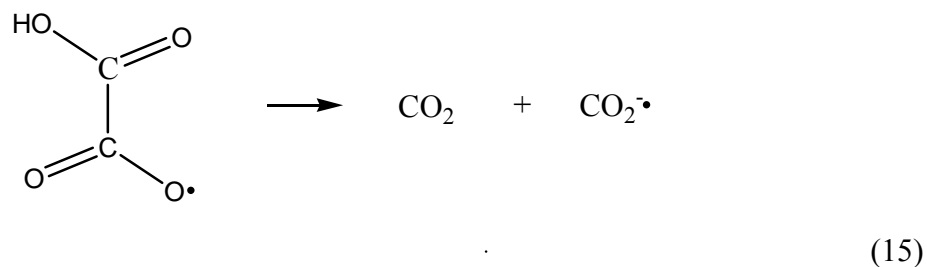
$$^{\text{US}}k_{\text{-ox}} = k[\cdot\text{OH}]_{\text{ss}}[\text{HC}_2\text{O}_4^-]_{\text{ss}} \quad (13)$$

Given equation 13 for $^{\text{US}}k_{\text{-ox}} = 1.4 \times 10^{-8} \text{ M s}^{-1}$, $k = 4.7 \times 10^7 \text{ M}^{-1}\text{s}^{-1}$, and $[\text{HC}_2\text{O}_4^-]_{\text{ss}} = 8.1 \times 10^{-4} \text{ M}$, an apparent steady-state hydroxyl radical concentration of $3.3 \times 10^{-13} \text{ M}$ is calculated in the presence of ultrasonic irradiation alone.

Getoff et al.³⁰ investigated the reaction between HC_2O_4^- and $\cdot\text{OH}$ using pulse radiolysis in N_2O -saturated oxalate solutions. Their results indicate that the reaction occurs via a direct electron transfer mechanism



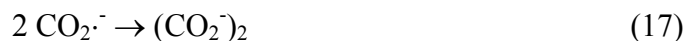
In the presence of oxygen, this radical intermediate undergoes bond cleavage and electron migration leading to the formation of CO_2 and a more stable carboxyl radical, $\text{CO}_2^{\cdot-}$.²⁸



The acidity of $\cdot\text{CO}_2\text{H}$ is uncertain, however its pK_a is estimated^{48,49} to a range from 2.3 to 3.9; thus both $\cdot\text{CO}_2\text{H}$ or $\text{CO}_2\cdot^-$ are active in our system.



In oxygen-limited neutral or alkaline solutions, the recombination of the carboxyl anion radical in aqueous solution is known to re-generate oxalate.^{48,50}



In the presence of oxygen, however, $\cdot\text{CO}_2\text{H}$ and $\text{CO}_2\cdot^-$ are scavenged by O_2 .⁵⁰



Given that the pK_a of $\text{HO}_2\cdot$ is 4.8,⁵¹ $\cdot\text{O}_2^-$ will be rapidly protonated at pH 3. This species will self-react to produce hydrogen peroxide and oxygen as a termination step in the overall free-radical mechanism.

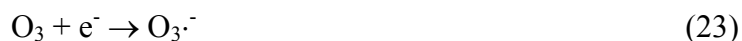


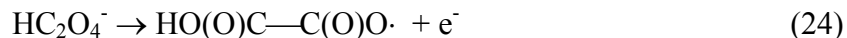
HC₂O₄⁻ Degradation with Ozone

Direct ozone attack on oxalate is relatively slow reaction as indicated by the bimolecular rate constants reported by Hoigne and Bader.³⁸ Thus, significant degradation by direct ozone attack is not expected.

$${}^2k[\text{O}_3 + \text{C}_2\text{O}_4^{2-} (\text{HC}_2\text{O}_4^-; \text{H}_2\text{C}_2\text{O}_4)] = 4.0 \times 10^{-2} (\ll 4.0 \times 10^{-2}) \text{ M}^{-1}\text{s}^{-1} \quad (22 \text{ a, b, c})$$

HC_2O_4^- is a saturated dicarboxylic acid that can only react with ozone directly via a one-electron transfer process. The redox couple for this proposed reaction is





The reduction potential for the O_3/O_3^- couple is 1.02 V.⁵² We have estimated the oxidation potential for reaction 24 to be -2.0 ± 0.2 V (see Appendix for further information). Therefore, we find the single-electron transfer reaction between O_3 and HC_2O_4^- to be thermodynamically unfavorable. However, the reduction potential for the $\cdot\text{OH}/\text{OH}^-$ couple is sufficiently high ($E \sim 1.9$ V^{53,54}) to favor the single electron transfer.

In addition to direct reactions with the solute, ozone decays in pure water to form a variety of secondary oxidants. This decomposition is initiated by OH^- attack and proceeds via a free radical pathway producing oxidants such as $\cdot\text{OH}$, $\text{HO}_2\cdot$, $\text{O}_2\cdot^-$ and $\text{O}_3\cdot^-$.^{51,55,56} Of these species, only $\cdot\text{OH}$ is expected to react with HC_2O_4^- via reaction 14.

Possible Mechanisms of Synergistic Action

As shown in Figure 3, the decomposition of HC_2O_4^- in the combined ultrasound/ozone system is significantly enhanced compared to treatment with either of the procedures alone. Degradation rates are proportional to both ozone concentrations and acoustic power, but at lower ozone concentrations there exists a critical acoustic power above which degradation is not enhanced further. An increase the ultrasonic power generally increases the number of cavitation events per unit time and the intensity of the individual bubble collapses, which increases the yield of $\cdot\text{OH}$, $\text{HO}_2\cdot$, $\cdot\text{O}_2^-$ and H_2O_2 ;^{42,57} However, this will also increase the sonolytic decomposition and degassing of ozone from solution.⁵⁸ As mentioned previously, oxalate is believed to only react with $\cdot\text{OH}$. Therefore, we considered two commonly accepted mechanisms that may account for the additional production of this radical species from ultrasonically irradiated ozone

solutions. Based on the results of this investigation, we also propose a third mechanism (Mechanism III) to explain the observed synergism of ozone and ultrasound for the degradation of oxalate.

Mechanism I: ·OH production via sonochemical decomposition of O₃.

The pyrolytic decomposition of gaseous ozone within sonically induced cavitation bubbles is reported to decompose this species into molecular and singlet oxygen. Through a subsequent reaction with water, two hydroxyl radicals are produced.



Mechanism II: ·OH production via O₃/H₂O₂ reactions

In addition to generating ·OH and other free-radical species, the sonolysis of water is also known to produce significant concentrations of hydrogen peroxide.^{42,43,57,59} While H₂O₂ does not react directly with O₃, HO₂⁻ is known to degrade aqueous ozone.^{51,55} Staehelin and Hoigne⁵¹ have proposed that the reaction between HO₂⁻ and O₃ initiates a free radical chain which ultimately produces ·OH.



In Chapter 5 we found that the reaction between O₃ and HO₂⁻ does not produce free radicals, but proceeds via a hydride transfer into a closed-shell trioxide species, HO₃⁻



The reactivity of this intermediate species is not very well understood; however, initial reports have suggested that it may act as a mild oxidizing reagent.^{60,61}

Mechanism III: ·OH production via O₃ reactions with CO₂·⁻

With the combined system, we hypothesize that HC₂O₄⁻ will be converted to CO₂·⁻ via reactions 14-16, just as it was with sonolysis alone. However, in addition to reacting with O₂ via reaction 19, we propose that the carboxyl anion radical will also undergo electron transfer with ozone to produce the ozonide radical



followed by reaction 29 and 30 to re-generate ·OH. This mechanism establishes a radical chain process as illustrated in Figure 4.

Examination of the Proposed O₃/US Mechanisms

Mechanism I

The synergistic effects of aqueous ozonolysis combined with sonolysis for the degradation and mineralization of organic compounds are the subject of several publications.^{6,33-35,58} In addition, the sonolysis of ozone in water enhances the yield of H₂O₂ compared to O₂- saturated water.^{35,62} In the absence of scavengers, the predominant stable product of the sonolysis of water is H₂O₂ which results from the self-termination reactions of the hydroxyl and the hydroperoxyl radicals, respectively.



Using the production rates of H_2O_2 as an indirect measure of free radical production, these studies suggested that the enhanced OH production results from the thermal decomposition of ozone inside the cavitation bubbles (rxns 25 and 26).

To verify whether this mechanism could account for the enhanced degradation of HC_2O_4^- in the combined system, batch ozone decay experiments were conducted were performed in the absence and presence of both oxalic acid and ultrasonic irradiation. As shown in Figure 5, the silent (i.e., non-acoustic) decay of ozone ($[\text{O}_3]_0 \sim 100 \mu\text{M}$) in pure water at pH 5 results in a $\sim 25\%$ loss within the first hour. This decay followed zero-order kinetics with $d[\text{O}_3]/dt = 0.4 \mu\text{M min}^{-1}$. No decay was observed for solutions of ozone dissolved in pure water adjusted to pH 3 with perchloric acid. (Fig. 6) This observation is in agreement with current ozone kinetic models which propose that the decay of aqueous ozone is initiated by OH^- attack and proceeds via a free radical pathway.^{51,55} The addition of oxalic acid to an ozonated solution depressed the pH from ~ 5 to 3. As shown in Figure 6, oxalate accelerates the degradation of ozone; however, $\sim 87\%$ of the initial ozone remained in solution one hour after removing the saturating gas. Ozone decay follows apparent zero-order kinetics with a decay rate of $0.18 \mu\text{M/min}$. This finding is consistent with previous findings⁶³ which indicated minimal oxidation of oxalic acid by O_3 at pH 3.5.

Application of 358 kHz ultrasound at 10 W to a pure solution of ozone increased the initial rate of O_3 decay to $\sim 1.6 \mu\text{M min}^{-1}$. (Fig. 5) The combined system resulted in an exponential decrease of ozone with sonication time with an apparent first-order rate constant of $k_{1, -\text{O}_3} = 0.032 \text{ min}^{-1}$ over more than three half-lives. (358 kHz, 10 W, 16.7 WL^{-1}) (Fig. 7) Previous studies have also observed enhanced apparent first-order ozone

decay kinetics in the presence of ultrasonic irradiation and attributed this increased degradation to sonolytic degradation and degassing.^{35,57,64} The direct pyrolysis of gaseous ozone is expected to lead to zero-order degradation kinetics since ozone is present in relatively low concentrations in the feed gas ($O_3/O_2 < 0.05$) and cavitation dynamics are not expected to change significantly with changes in ozone concentration.⁶⁵ However, ozone also reacts with $\cdot OH$



The reported bimolecular rate constant for this reaction is $k_{34} = 1.1 \times 10^8 \text{ M}^{-1}\text{s}^{-1}$,⁶⁶ which suggests that reaction 34 would lead to increased ozone degradation in the bubble and in solutions. However, as ozone concentrations are reduced, this process would compete with the self-reaction of the hydroxyl radical (rxn 32, $k_{32} = 5.5 \times 10^9 \text{ M}^{-1}\text{s}^{-1}$ rxn 32), resulting in the apparent first-order degradation kinetics for ozone.

As noted above, oxalate does not react significantly with ozone. In addition, the presence of oxalate is not expected to enhance the cavitation efficiency of the acoustic field. If the enhanced production of $\cdot OH$ in the sonolytic ozone system resulted only from the pyrolytic decomposition of ozone, then ozone decomposition in the experiments should not vary significantly with the addition of oxalic acid. In addition, if ozone decomposition also results from $\cdot OH$ attack in solution (rxn 34), then the presence of oxalic acid could compete for this radical species via reaction 14, decreasing the observed ozone decay rates. However, results shown in Figure 8 indicate that the simultaneous addition of oxalic acid with the application of the ultrasonic irradiation led to an initial O_3 decay rate of $3.5 \mu\text{M min}^{-1}$, more than doubling the loss rate compared with sonication

alone. In addition to enhancing the rate of ozone loss, the presence of oxalic acid also changed the overall kinetics of the reaction from apparent first-order to zero-order.

These findings are not entirely consistent with mechanism I. However, mechanism III, which is illustrated in Figure 4, may resolve this discrepancy. In mechanism III, ozone reacts with $\text{CO}_2^{\cdot-}$ via reaction 31, and subsequently produces an additional $\cdot\text{OH}$ (rxns 29 and 30). Since oxalate is in 10-fold excess compared with ozone, the steady-state concentration of $\cdot\text{OH}$ in solution is increased to a higher level over the duration of the experiment. $\cdot\text{OH}$ is then able to either directly react with ozone via reaction 34 or cycle through the chain mechanism shown in Figure 4.

Mechanism II

Kang and Hoffmann⁶⁷ also found mechanism I to be insufficient to account for their observations during the combined ozonolysis and ultrasonic irradiation of methyl tert-butyl ether. They proposed that in addition to the direct pyrolysis of ozone, the additional reactivity in the combined system may also arise from additional ozone reactions with sonically generated H_2O_2 . Experiments performed in identical ultrasonic reactors operating with similar power densities and frequencies to our system have estimated the sonochemical production rate of hydrogen peroxide in pure water to be between 1.5 and 3 $\mu\text{M min}^{-1}$.^{43,57} Previous research has indicated that in the absence of ultrasonic irradiation, the direct addition of H_2O_2 to water saturated with O_3 increases the solution's relative reactivity and ability to oxidize a number of other organic substrates^{56,68-70} including oxalic acid.^{63,71} The enhanced reactivity of these systems has been attributed the production $\cdot\text{OH}$ via the reactions 27-30.

To assess the additional reactivity resulting from the sonochemically generated H_2O_2 , batch ozone solutions were prepared under simultaneous low-power ultrasonic irradiation. These comparative results are shown in Figures 5 and 9. It is clear that ozone decomposition in pure water was significantly faster with pre-sonication compared to solutions prepared under acoustically “silent” conditions. With continuous ultrasonic irradiation, initial decay rates follow zero-order kinetics with $-\text{d}[\text{O}_3]/\text{dt} \sim 6.4 \mu\text{M min}^{-1}$. Pre-sonication increased the ozone decay rate nearly four times compared to solutions irradiated only after the removal of the ozone source. This accelerated decomposition remained for the first 10 minutes of reaction, after which rates significantly slowed and exponential decay kinetics were re-established. Nearly identical initial decay kinetics were also measured in this system when sonolysis was halted concurrently with the removal of the feed gas. However, the rapid initial loss of ozone stops after 10 minutes and the decay rate over the next hour was reduced to $-\text{d}[\text{O}_3]/\text{dt} \sim 0.14 \mu\text{M min}^{-1}$. (Fig. 9)

These findings indicate that relatively long-lived intermediate products capable of reacting with ozone are formed during the ultrasonic irradiation of ozone saturated solutions. We believe HO_2^- which results from the dissociation of sonically generated H_2O_2 is also reacting with the ozone via reactions 27-30 or possibly via reaction 27 a. In Chapter 5 we found the stoichiometry of the peroxone reaction to vary between $\Delta\text{O}_3/\Delta\text{H}_2\text{O}_2 = 2.7$ and 7.1. Figure 9 indicates a loss of $\sim 70 \mu\text{M O}_3$ which corresponds to $[\text{H}_2\text{O}_2]_0$ between 10 and 25 μM . These H_2O_2 concentrations are consistent with the findings of Kang and Hoffmann.⁶⁷

As shown in Figure 10, the addition of oxalic acid to pre-sonicated batch solution enhanced the ozone decay mechanism when irradiation continued during the experiment.

While initial decay rates were not altered significantly, enhanced degradation was observed after 10 minutes of insonation. As discussed in the previous section, this additional reactivity can be attributed to the enhanced production of $\cdot\text{OH}$ resulting from the reactions described in mechanism III. However, when sonolysis was halted concurrently with the start of the kinetic run, the presence of oxalate actually inhibited the degradation of ozone compared to experiments performed in neat water. (Fig. 11) This observation is most likely not the result of a competitive reaction between HC_2O_4^- for reactive species generated by the sonozone treatment, but rather can be attributed to the pH drop within the solution from pH 5 to ~ 3 upon addition of $\text{H}_2\text{C}_2\text{O}_4$. This increase in acidity effectively lowers the $[\text{HO}_2^-]_{\text{ss}}$ by two orders of magnitude, significantly slowing the degradation of ozone by reactions 27-30 or reaction 27a.

In an effort to determine whether additional $\text{H}_2\text{O}_2/\text{O}_3$ reactions could account for the strong synergism of the combined system for the oxidation of HC_2O_4^- , separate oxalate degradation experiments were performed using pre-sonicated ozone solutions. Ozone saturated water $[\text{O}_3]_{\text{ss}} = 150 \mu\text{M}$ was irradiated at 358 kHz at several acoustic powers ranging from 0-100 watts for an hour prior to the addition of oxalate. Degradation rates in the pre-sonicated solutions were nearly identical to the rates obtained when ultrasonic irradiation commenced at $t = 0$. (Fig 12). A similar lack of enhancement is shown in Figure 13, when H_2O_2 was spiked along with oxalic acid to a combined ozone/ultrasound system. (358 kHz, 100 W, $[\text{O}_3]_{\text{ss}} = 150 \mu\text{M}$, $[\text{H}_2\text{O}_2]_0 = 50, 112, \text{ and } 300 \mu\text{M}$. $[\text{H}_2\text{C}_2\text{O}_4]_0 = 0.9 \text{ mM}$) Figure 13 also indicates that at excessive ($\sim 2 \text{ mM}$) concentrations of H_2O_2 , the degradation of HC_2O_4^- can actually be inhibited. This

is the result of $\cdot\text{OH}$ scavenging by H_2O_2 to produce the essentially unreactive hydroperoxyl radical, $\text{HO}_2\cdot$.



The bimolecular rate constant of this reaction is reported⁷² as $k_{35} = 2.7 \times 10^7 \text{ M}^{-1}\text{s}^{-1}$. The scavenging of $\cdot\text{OH}$ from solution therefore only becomes competitive with the reaction between $\cdot\text{OH}$ and HC_2O_4^- ($k_{11b} = 4.7 \times 10^7 \text{ M}^{-1}\text{s}^{-1}$) when $[\text{H}_2\text{O}_2]_0 \geq 1.5 \text{ mM}$, which is agreement with our experimental findings.

In the absence of ultrasonic irradiation, the simultaneous addition of oxalic acid and H_2O_2 to water saturated with ozone did enhance the degradation of bioxalate. (Fig. 14) The addition of 300 and 2000 μM H_2O_2 to an ozone saturated solutions ($[\text{O}_3]_{\text{ss}} = 350 \mu\text{M}$) increased degradation rates nearly 10-fold compared to simple ozonolysis, with an average normalized pseudo zero-order rate constant of $^{\text{H}_2\text{O}_2\text{-O}_3}k'_{-\text{ox}} = 1.0 \times 10^{-2} \text{ min}^{-1}$. It is believed that this process is the result of the produced via rxn 27a (See Chapter 5). The reactivity of HO_3^- is still being evaluated. These findings suggest that in the absence of steady production of $\cdot\text{OH}$ from sonochemical reactions, the degradation of oxalate is enhanced in a combined $\text{H}_2\text{O}_2/\text{O}_3$ solution.

Mechanism III

Additional support for mechanism III was recently reported by Lind et al.⁷³ Their work provided evidence for the direct reaction between $\text{CO}_2\cdot^-$ and O_3 during the γ -radiolysis of ozonated solutions of formate. The reduction potential for CO_2 going to the carbon dioxide radical, $\text{CO}_2\cdot^-$, has been determined to be $\sim -1.8 \text{ V}$.^{74,75} Considering that

the single-electron reduction potential for ozone to the ozonide radical, $O_3^{\cdot-}$ (rxn 23) is 1.02 V,⁵² the redox couple for this proposed reaction



would be thermodynamically favorable and should lead to the enhanced production of $\cdot OH$.

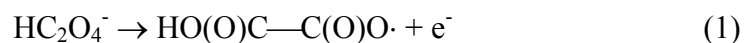
Conclusions

This study demonstrates that the combination of ozonolysis and ultrasound is able to degrade aqueous oxalate more efficiently than predicted by the simple linear addition of two independently reacting systems. Ozone decay experiments suggest that the apparent rate enhancements are the result of a reaction between the carbon dioxide radical anion and molecular ozone. This reaction effectively increases the yield of hydroxyl radical which is known to rapidly oxidize oxalate.

Appendix

Thermochemical Considerations

The oxidation half-reaction of bioxalate to its corresponding radical is given by



The oxidation potential for reaction 1, E_1 can be expressed as

$$E_1 = \frac{-\Delta_r G_1}{nF} \quad (2)$$

where n is the number of electrons, and F is the Faraday constant, and $\Delta_r G_1$ is the standard Gibbs energy for reaction 1. $\Delta_r G_1$ is given by the difference in standard Gibbs energies, $\Delta_f G$, of the products and the reactants

$$\Delta_r G_1 = \Delta_f G (\text{HO(O)C—C(O)O}\cdot) - \Delta_f G (\text{HC}_2\text{O}_4^-) \quad (3)$$

We can estimate the value of $\Delta_r G_1$ as follows:

The H-bond dissociation of oxalic acid will produce the bioxalate radical



The acid-dissociation of oxalic acid will yield bioxalate



An electron transfer from bioxalate to a proton will also produce the bioxalate radical



From the above reactions the following relationship is obtained:

$$\Delta_r G_1 = \Delta_r G_6 - \Delta_f G (\text{H}\cdot) + \Delta_f G (\text{H}^+) = \Delta_r G_4 - \Delta_r G_5 - \Delta_f G (\text{H}\cdot) + \Delta_f G (\text{H}^+) \quad (7)$$

where $\Delta_f G (\text{H}^+) = 0 \text{ kJ mol}^{-1}$,⁷⁶ $\Delta_f G (\text{H}\cdot) = 203.25 \text{ kJ mol}^{-1}$,⁷⁶ $\Delta_r G_4 \sim 405 \text{ kJ mol}^{-1}$ and $\Delta_r G_5 \sim 7.0 \text{ kJ mol}^{-1}$ (see calculations for $\Delta_r G_4$ and $\Delta_r G_5$ at the end of this discussion).

From eq. 7, we estimate $\Delta_r G_1 = 195 \text{ kJ mol}^{-1}$. Given eq. 2 with $F = 96,485 \text{ C mol}^{-1}$, $n = 1$, and $\Delta_r G_1 = 195 \text{ kJ mol}^{-1}$, we calculate that $E_1 = 2.0 \text{ V}$.

Calculating $\Delta_r G_4$

The standard Gibbs energy for reaction 4, $\Delta_r G_4$, can be expressed as

$$\Delta_r G_4 = \Delta_r H_4 - T\Delta_r S_4 \quad (8)$$

where $\Delta_r H_4$ is the enthalpy for reaction 4, $\Delta_r S_4$ is the entropy of reaction 4, and T is the temperature. $\Delta_r H_4$ can be approximated by considering the H-bond dissociation energy of acetic acid, $\Delta_r H_4 \sim \Delta H_{\text{BDE}}(\text{CH}_3\text{CO}_2\text{H}) = 442.2 \text{ kJ mol}^{-1}$ ⁷⁷. The change in entropy in reaction 1 should not vary significantly from the entropy changes observed in the H-bond dissociation of formic acid as follows:

$$\Delta_r S_4 \sim \Delta_r S_{\text{BDE}}(\text{HCOOH}) = \Delta S(\text{HCOO}\cdot) + \Delta S(\text{H}\cdot) - \Delta S(\text{HCOOH}) \quad (9)$$

where $\Delta S(\text{HCOO}\cdot) = 248.3 \text{ J K}^{-1}\text{mol}^{-1}$,⁷⁸ $\Delta S(\text{H}\cdot) = 114.7 \text{ J K}^{-1}\text{mol}^{-1}$,⁷⁶ and $\Delta S(\text{HCOOH}) = 239.5 \text{ J K}^{-1}\text{mol}^{-1}$.⁷⁸ Thus, $\Delta_r S_4 = 123.5 \text{ J K}^{-1}\text{mol}^{-1}$. Furthermore, with $\Delta_r H_4 = 442.2 \text{ kJ mol}^{-1}$, $\Delta_r S_4 = 123.5 \text{ J K}^{-1}\text{mol}^{-1}$ and $T = 298 \text{ K}$, we estimate $\Delta_r G_4 = 405 \text{ kJ mol}^{-1}$.

Calculating $\Delta_r G_5$

The Gibb's free energy of reaction 5 is related to the acid equilibrium constant, K_a , by

$$\Delta_r G_5 = -RT \ln K_a \quad (10)$$

With the $\text{p}K_a = 1.23$, $K_a = 0.059$ and with $R = 8.3145 \text{ J K}^{-1}\text{mol}^{-1}$, and $T = 298 \text{ K}$, we obtain $\Delta_r G_5 = 7.02 \text{ kJ mol}^{-1}$.

References

- (1) Legrand, M.; DeAngelis, M. *J. Geophys. Res. - Atmos.* **1996**, *101*, 4129.
- (2) Smith, R.; Oremland, R. *Appl. Environ. Microb.* **1983**, *46*, 106.
- (3) Edwards, M.; Benjamin, M. *J. Am. Waterworks Assoc.* **1992**, *84*, 56.
- (4) Stern, M.; Heinzle, E.; Kut, O.; Hungerbuhler, K. *Water Sci. Technol.* **1997**, *35*, 329.
- (5) Stockinger, H.; Heinzle, E.; Kut, O. *Environ. Sci. Technol.* **1995**, *29*, 2016.
- (6) Weavers, L.; Malmstadt, N.; Hoffmann, M. *Environ. Sci. Technol.* **2000**, *34*, 1280.
- (7) Kotronarou, A.; Mills, G.; Hoffmann, M. *J. Phys. Chem.* **1991**, *95*, 3630.
- (8) Liakou, S.; Kornaros, M.; Lyberatos, G. *Water Sci. Technol.* **1997**, *36*, 155.
- (9) Vinodgopal, K.; Peller, J. *Res. Chem. Intermed.* **2003**, *29*, 307.
- (10) Hara, K.; Osada, K.; Matsunaga, K.; Sakai, T.; Iwasaka, Y.; Furuya, K. *J. Geophys. Res. - Atmos.* **2002**, *107*, article number 4399.
- (11) Stock, N.; Peller, J.; Vinodgopal, K.; Kamat, P. *Environ. Sci. Technol.* **2000**, *34*, 1747.
- (12) Colarusso, P.; Serpone, N. *Res. Chem. Intermediat.* **1996**, *22*.
- (13) Bhandari, A.; Koul, S.; Sekhon, A.; Pramanik, S.; Chaturvedi, L.; Huang, M.; Menon, M.; Koul, H. *J. Urology* **2002**, *168*, 253.
- (14) Miller, C.; Kennington, L.; Cooney, R.; Kohimoto, Y.; Cao, L.; Honeyman, T.; Pullman, J.; Jonassen, J.; Scheid, C. *Toxicol. Appl. Pharm.* **2000**, *162*, 132.
- (15) Jonassen, J.; Cao, L.; Honeyman, T.; Scheid, C. *Crit. Rev. Euk. Gene Expr.* **2003**, *13*, 55.

- (16) Allison, M.; Cook, H. *Science* **1981**, *212*, 675.
- (17) Saffir, P.; Taube, H. *J. Am. Chem. Soc.* **1960**, *82*, 13.
- (18) Jones, T.; Noyes, R. *J. Phys. Chem.* **1983**, *87*, 4686.
- (19) Reckley, J.; Show Alter, K. *J. Am. Chem. Soc.* **1981**, *103*, 7012.
- (20) Allen, T. *J. Am. Chem. Soc.* **1951**, *73*, 3589.
- (21) Knoller, Y.; Perlmutter-Hayman, B. *J. Am. Chem. Soc.* **1955**, *77*, 3212.
- (22) Domenech, J.; Peral, J. *J. Chem. Res. - S* **1987**, *11*, 360.
- (23) Beltran, F.; Rivas, F.; Montero-de-Espinoza, R. *Ind. Eng. Chem. Res.* **2003**, *42*, 3210.
- (24) Pines, D.; Reckhow, D. *Environ. Sci. Technol.* **2002**, *36*, 4046.
- (25) Beltran, F.; Rivas, F.; Montero-de-Espinoza, R. *Ind. Eng. Chem. Res.* **2003**, *42*, 3218.
- (26) Andreozzi, R.; Insola, A.; Caprio, V.; Marotta, R.; Tufano, V. *Appl. Catal. A - Gen.* **1996**, *138*, 75.
- (27) Andreozzi, R.; Caprio, V.; Insola, A.; Marotta, R.; Tufano, V. *Ind. Eng. Chem. Res.* **1997**, *36*, 4774.
- (28) Draganic, Z.; Draganic, I.; Dosanic, M. *J. Phys. Chem.* **1964**, *68*, 2085.
- (29) Draganic, Z.; Draganic, I.; Kosanic, M. *J. Phys. Chem.* **1966**, *70*, 1418.
- (30) Getoff, N.; Schworer, F.; Markovic, V.; Sehested, K.; Nielsen, O. *J. Phys. Chem.* **1971**, *75*, 749.
- (31) Peller, J.; Wiest, O.; Kamat, P. *J. Phys. Chem. A* **2001**, *105*, 3176.
- (32) Naffrechoux, E.; Chanoux, S.; Petrier, C.; Suptil, J. *Ultrasonics Sonochemistry* **2000**, *7*, 255.

- (33) Destailats, H.; Colussi, A.; Joseph, J.; Hoffmann, M. *J. Phys. Chem. A* **2000**, *104*, 8930.
- (34) Olson, T.; Barbier, P. *Water Res* **1994**, *28*, 1383.
- (35) Barbier, P.; Petrier, C. *J. Adv. Oxid. Technol.* **1996**, *1*, 154.
- (36) Hung, H. M.; Hoffmann, M. R. *J. Phys. Chem.* **1999**, *103*, 2734.
- (37) Smith, R.; Kilford, J. *Int. J. Chem. Kinet.* **1976**, *8*, 1.
- (38) Hoigne, J.; Bader, H. *Water Res.* **1983**, *17*, 185.
- (39) Elliot, A.; Buxton, G. *J. Chem. Soc. Faraday T.* **1992**, *88*, 2465.
- (40) Bielski, B.; Cabelli, D.; Arudi, R.; Ross, A. *J. Phys. Chem. Ref. Data* **1985**, *14*, 1041.
- (41) Buxton, G.; Greenstock, C.; Helman, W.; Ross, A. *J. Phys. Chem. Ref. Data* **1988**, *17*, 513.
- (42) Mason, T.; Lorimer, J. *Applied Sonochemistry. The Uses of Power Ultrasound in Chemistry and Processing*; Wiley-VCH: Weinheim, Germany, 2002.
- (43) Hua, I.; Hoffmann, M. *Environ. Sci. Technol.* **1997**, *31*, 2237.
- (44) Bielski, B.; Richter, H. W. *J. Am. Chem. Soc.* **1977**, *99*, 3019.
- (45) Beckett, M.; Hua, I. *Environ. Sci. Technol.* **2000**, *34*, 3944.
- (46) Joseph, J.; Destailats, H.; Hung, H.; Hoffmann, M. *J. Phys. Chem. A* **2000**, *104*, 301.
- (47) Destailats, H.; Lesko, T.; Knowlton, M.; Wallace H; Hoffmann, M. *Ind. Eng. Chem. Res.* **2001**, *40*, 3855.
- (48) Flyunt, R.; Schuchmann, M.; von Sonntag, C. *Chem. - Eur. J.* **2001**, *7*, 796.
- (49) Fojtik, A.; Czapski, G.; Henglein, J. *J. Phys. Chem.* **1970**, *74*, 3204.

- (50) Hart, E.; Henglein, A. *J. Phys. Chem.* **1985**, *89*, 4342.
- (51) Staehelin, J.; Hoigne, J. *Environ. Sci. Technol.* **1982**, *16*, 676.
- (52) Bennett, L.; Warlop, P. *Inorg. Chem.* **1990**, *29*, 1975.
- (53) Schwarz, H.; Dodson, R. *J. Phys. Chem.* **1984**, *88*, 3643.
- (54) Klaning, U.; Sehested, K.; Holcman, J. *J. Phys. Chem.* **1985**, *89*, 5271.
- (55) Staehelin, J.; Hoigne, J. *Environ. Sci. Technol.* **1979**, *16*, 676.
- (56) Gottschalk, C.; Libra, J.; Saupe, A. *Ozonation of Water and Waste Water. A Practical Guide to Understanding Ozone and its Application*; Wiley-VCH: New York, 2000.
- (57) Kang, J.; Hung, H.; Lin, A.; Hoffmann, M. *Environ. Sci. Technol.* **1999**, *33*, 3199.
- (58) Weavers, L.; Ling, F.; Hoffmann, M. *Environ. Sci. Technol.* **1998**, *18*, 2727.
- (59) Petrier, C.; Francony, A. *Ultrasonics Sonochemistry* **1997**, *4*, 295.
- (60) Wentworth, P.; Wentworth, A.; Zhu, X.; Wilson, I.; Janda, K.; Eschenmoser, A.; Lerner, R. *Proc. Natl. Acad. Sci.* **2003**, *100*, 1490.
- (61) Xu, X.; Goddard, G. I. *Proc. Natl. Acad. Sci.* **2002**, *99*, 15308.
- (62) Hart, E.; Henglein, A. *J. Phys. Chem.* **1986**, *90*, 3061.
- (63) Brunet, R.; Bourbigot, M.; Dore, M. *Ozone Sci. Eng.* **1984**, *6*, 163.
- (64) Weavers, L.; Hoffmann, M. *Environ. Sci. Technol.* **1998**, *32*, 3941.
- (65) Colussi, A.; Hoffmann, M. *J. Phys. Chem. A* **1999**, *103*, 2696.
- (66) Sehested, K.; Holcman, J.; Bjergbakke, E.; Hart, E. *J. Phys. Chem.* **1984**, *88*, 4144.
- (67) Kang, J.; Hoffmann, M. *Environ. Sci. Technol.* **1998**, *32*, 3194.
- (68) Acero, J.; Von Gunten, U. *J. Am Water Works Ass.* **2001**, *October*, 90.

- (69) Elovitz, M.; von Gunten, U. *Ozone Sci. Eng.* **1999**, *21*, 239.
- (70) Elovitz, M.; von Gunten, U.; Kaiser, H. *Ozone Sci. Eng.* **2000**, *22*, 123.
- (71) Paillard, H.; Brunet, R.; Dore, M. *Water Res.* **1988**, *22*, 91.
- (72) Christensen, H.; Sehested, K.; Corfitzen, H. *J. Phys. Chem.* **1982**, *86*, 1588.
- (73) Lind, J.; Merenyi, G.; Hohansson, E.; Brink, T. *J. Phys. Chem.* **2003**, *107*, 676.
- (74) Surdhar, P.; Mezyk, S.; Armstrong, D. *J. Phys. Chem.* **1989**, *93*, 3360.
- (75) Koppenol, W.; Rush, J. *J. Phys. Chem.* **1987**, *16*, 4429.
- (76) Atkins, P. *Physical Chemistry*, 5 ed.; W.H. Freeman and Company: New York, 1994.
- (77) Colussi, A. *Chemical Kinetics of Small Organic Radicals.*; Alfassi, Z, Ed.; CRC Press: Boca Raton, Fl, 1988; Vol. 1; pp 150.
- (78) Benson, S. *Thermochemical Kinetics*, 2 ed.; Wiley: New York, 1976.

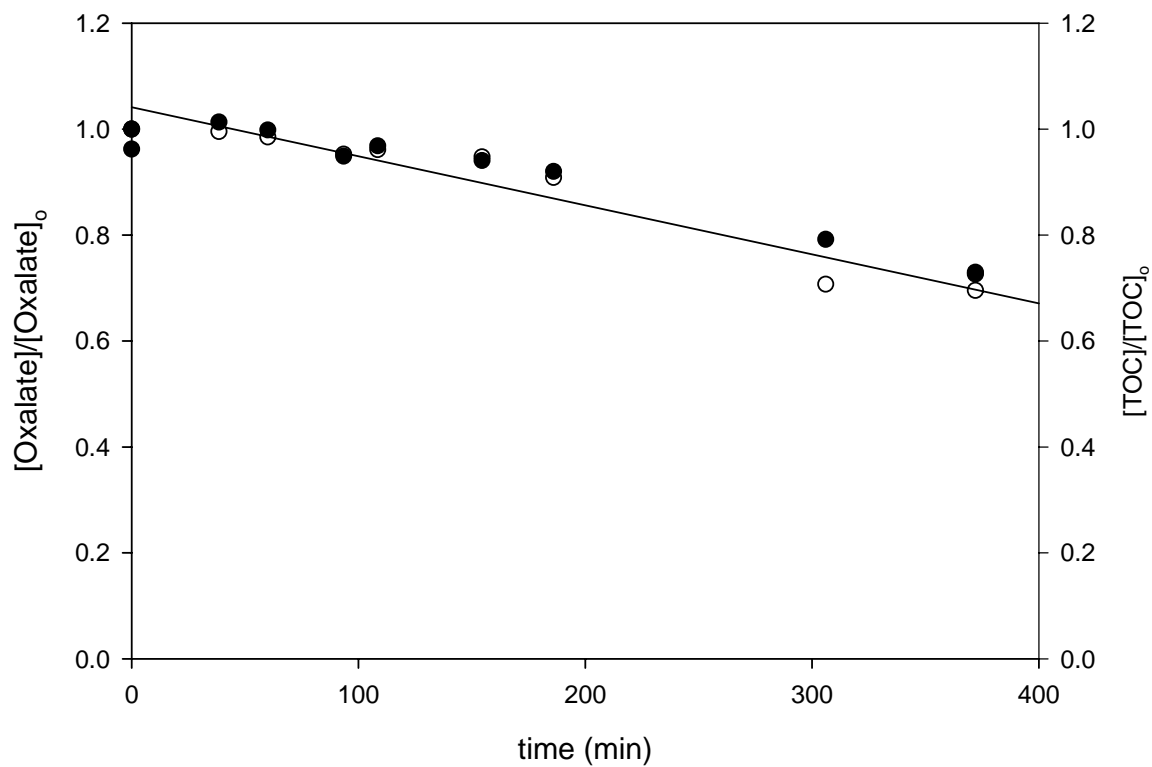


Figure 1. Degradation of $[H_2C_2O_4]_t$ with ultrasound ($[H_2C_2O_4]_0 = 0.9$ mM, 358 kHz, 100 W, 0.605 L, 15 °C, pH ~ 3). o: normalized oxalate concentrations; •: normalized TOC concentrations

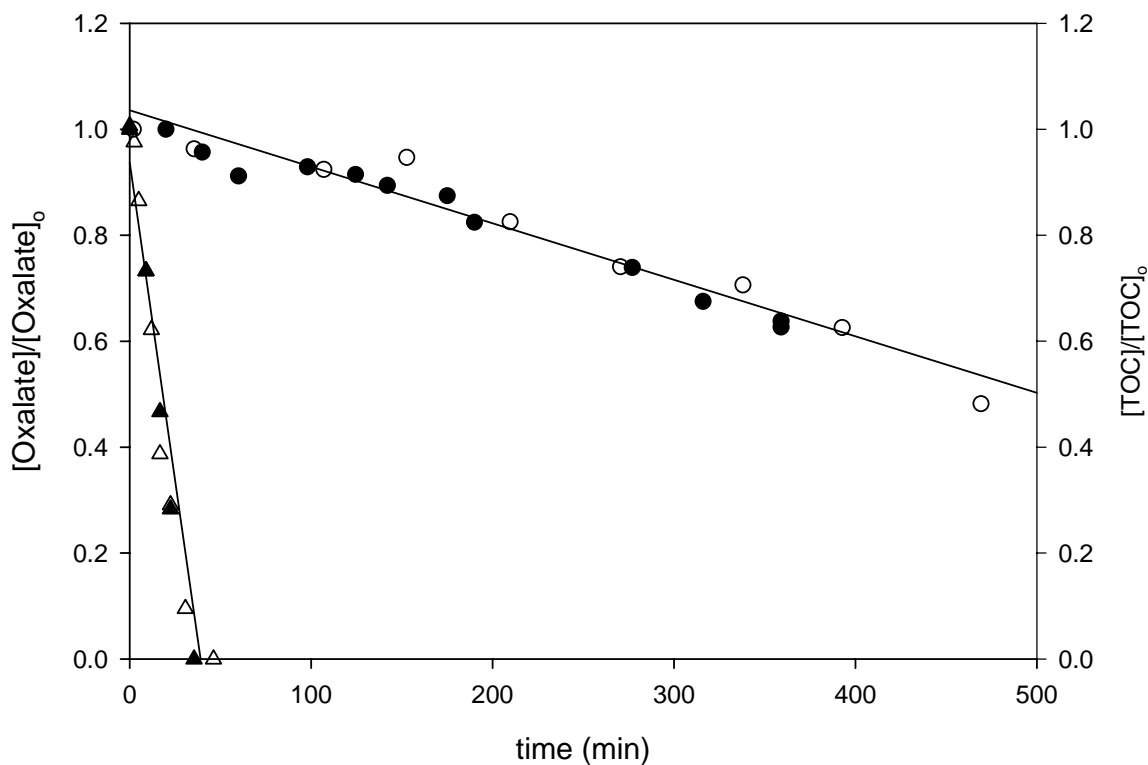


Figure 2. Degradation of $[\text{H}_2\text{C}_2\text{O}_4]_t$ with ozone and ozone/ultrasound ($[\text{H}_2\text{C}_2\text{O}_4]_0 = 0.9$ mM, 0.605 L, 15 °C, pH ~ 3). ○: normalized oxalate concentrations using ozone only ($[\text{O}_3]_{\text{ss}} = 340$ μM); ●: normalized TOC concentrations using ozone only ($[\text{O}_3]_{\text{ss}} = 340$ μM); Δ: normalized oxalate concentrations using ozone with ultrasound ($[\text{O}_3]_{\text{ss}} = 350$ μM , 358 kHz, 100 W); ▲: normalized TOC concentrations using ozone with ultrasound ($[\text{O}_3]_{\text{ss}} = 350$ μM , 358 kHz, 100 W);

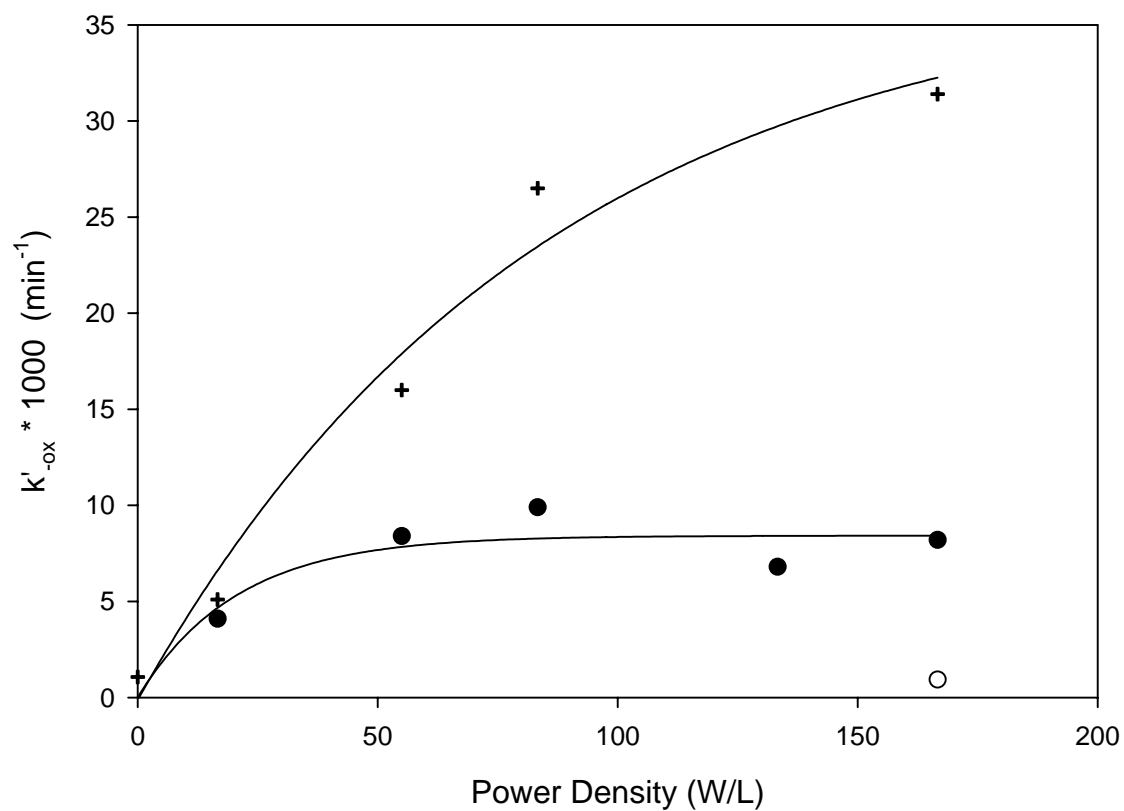


Figure 3. Normalized pseudo zero-order degradation rate constants of $[\text{H}_2\text{C}_2\text{O}_4]_t$ versus ultrasonic power density (358 kHz, 0.605 L, $[\text{C}_2\text{H}_4\text{O}_4]_o = 0.9$ mM, 0.605 L, 15 °C, pH ~ 3). +: $[\text{O}_3]_{ss} = 350$ μM; •: $[\text{O}_3]_{ss} = 150$ μM; o: $[\text{O}_3]_{ss} = 0$ μM.

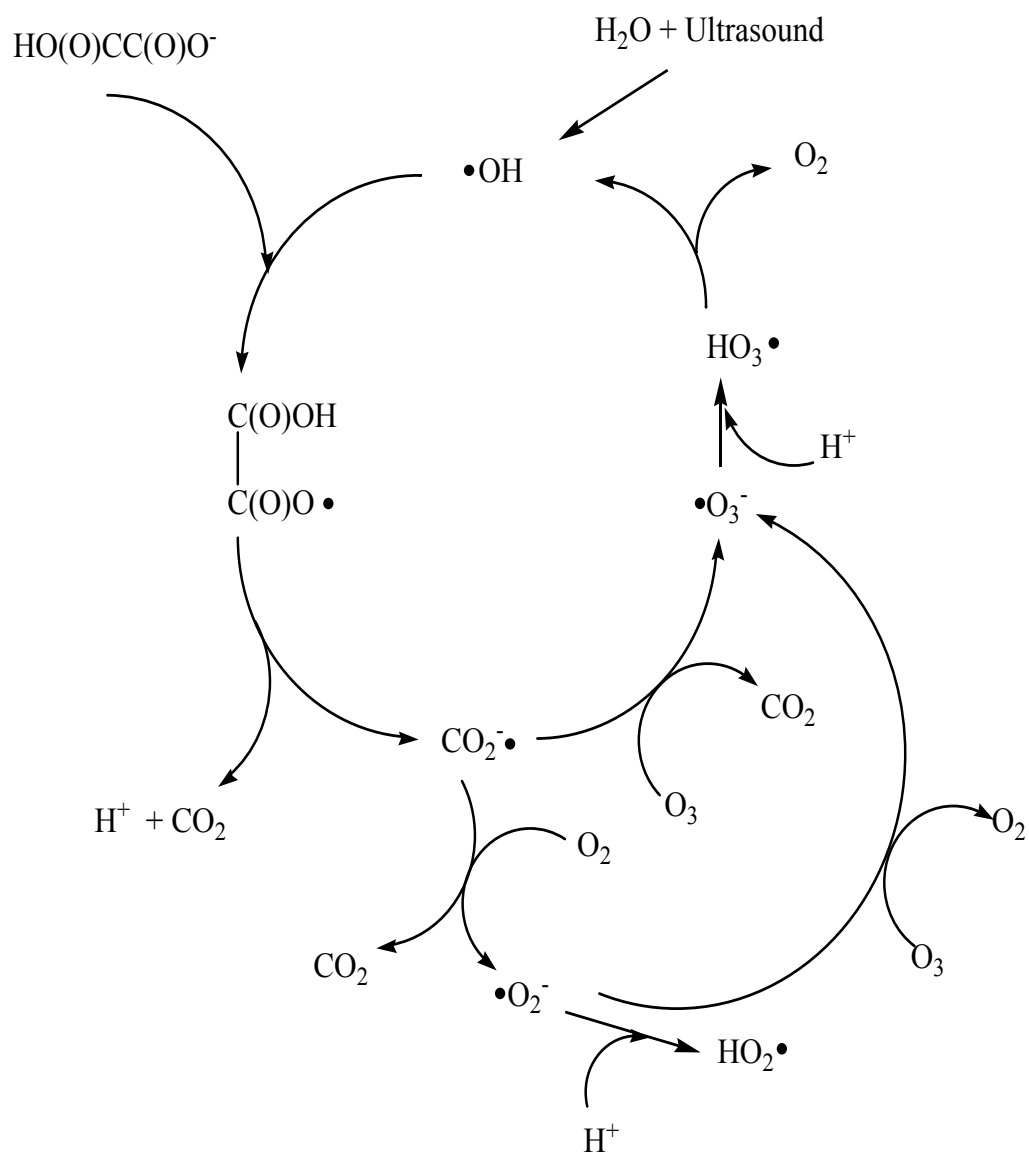


Figure 4: Proposed free chain reaction for $O_3 + HC_2O_4^-$ (Mechanism III).

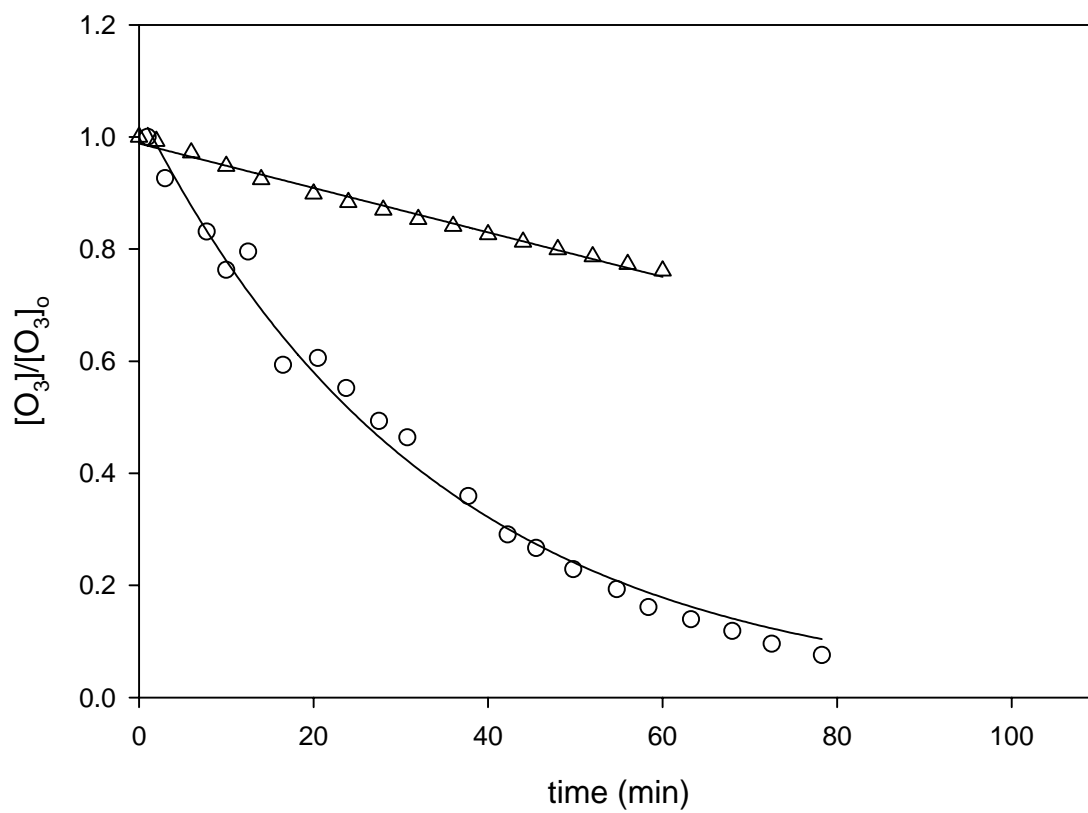


Figure 5: Ozone decay in ultrapure water ($[O_3]_0 = 100 \mu\text{M}$, 0.605 L, 15 °C, $\text{pH}_{\text{initial}} \sim 5$). Δ : in pure water; \circ : ultrasound is applied at $t = 0$ (358 kHz, 10 W)

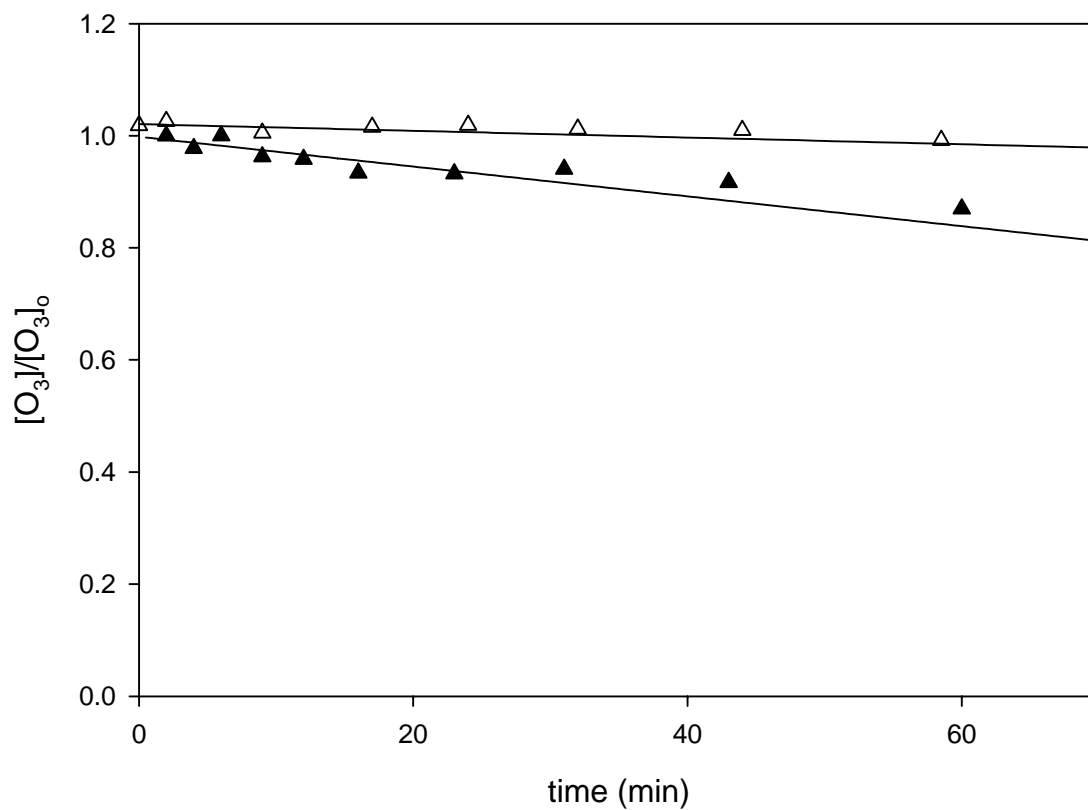


Figure 6: Ozone decay in ultrapure water. ($[O_3]_0 = 100 \mu\text{M}$, 0.605 L, 15 °C, $\text{pH}_{\text{initial}} \sim 3$). Δ : in pure water; \blacktriangle : oxalic acid is added at $t = 0$ ($[H_2C_2O_4]_0 = 0.9 \text{ mM}$)

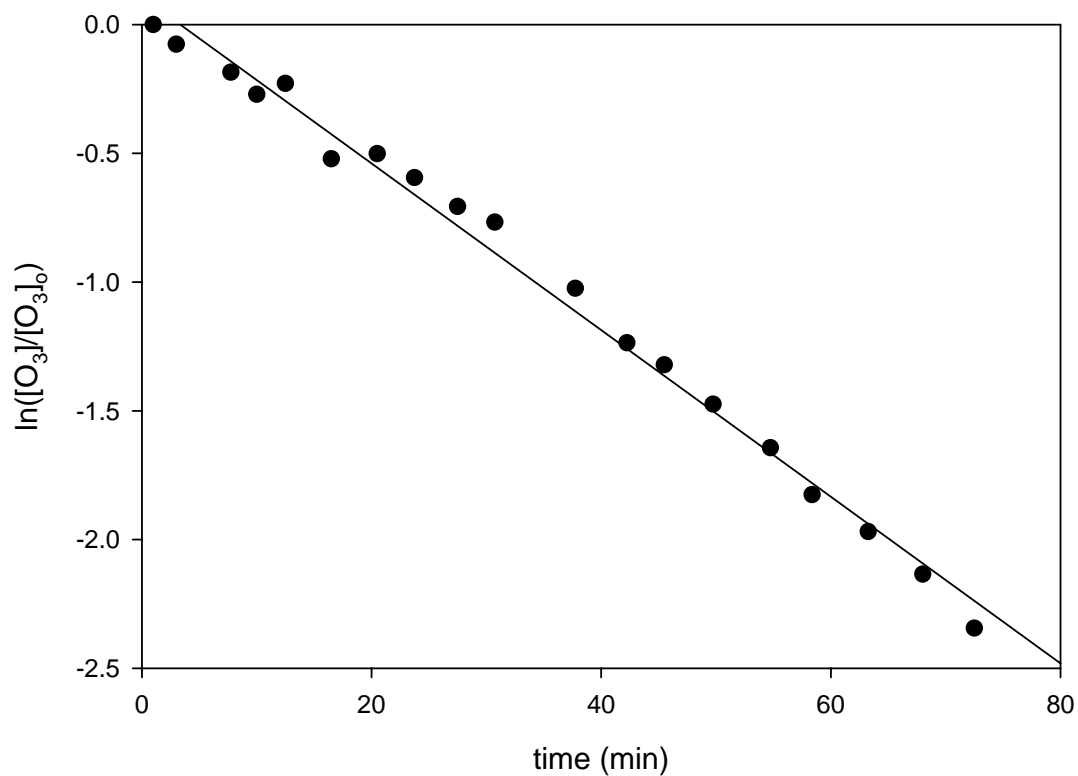


Figure 7: Ozone decay in ultrapure water when ultrasound is applied at $t = 0$ ($[O_3]_0 = 100 \mu\text{M}$, 358 kHz, 10 W, 0.605 L, 15 °C, $\text{pH}_{\text{initial}} \sim 5$).

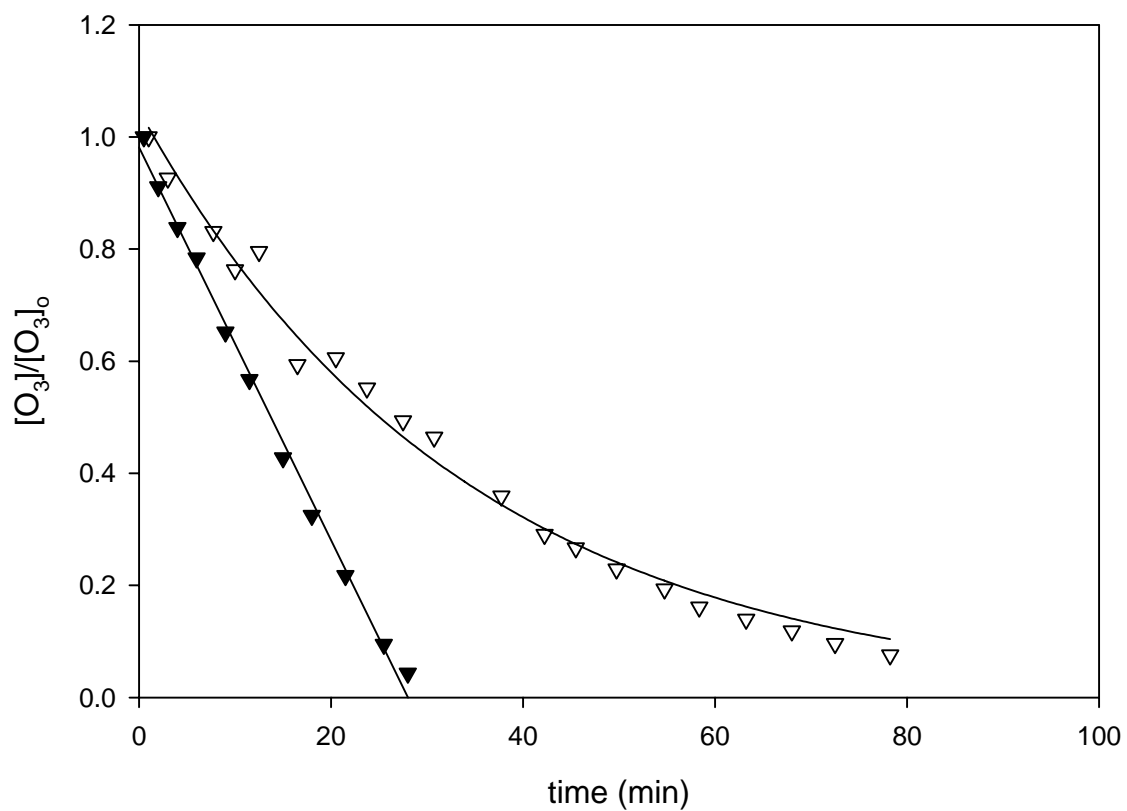


Figure 8: Ozone decay in ultrapure water in the presence of ultrasound irradiation applied at $t = 0$. ($[O_3]_0 = 100 \mu\text{M}$, 358 kHz, 10 W, 15 °C) ∇ : in neat water ($\text{pH}_{\text{initial}} \sim 5$); \blacktriangledown : $[\text{H}_2\text{C}_2\text{O}_4]_0 = 0.9 \text{ mM}$ added at $t = 0$ ($\text{pH}_{\text{initial}} \sim 3$)

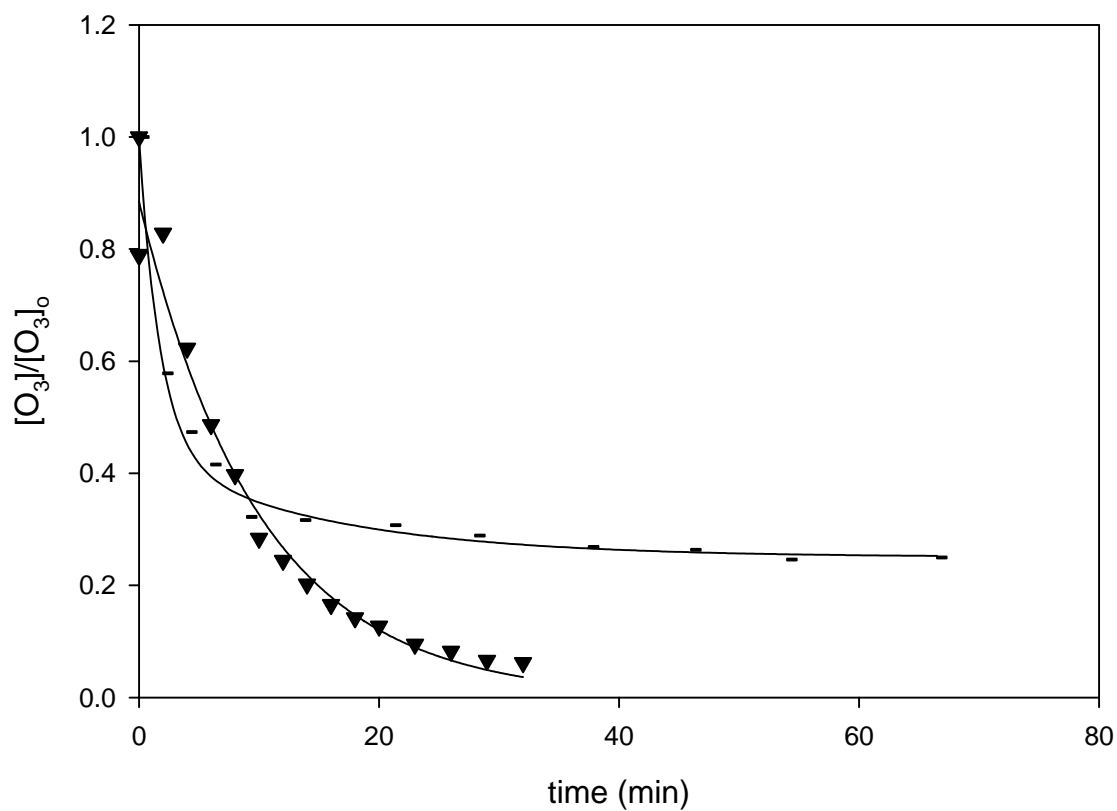


Figure 9: Ozone decay in ultrapure water. Ozone solution is pre-sonicated for 1 hour prior to $t=0$ ($[O_3]_0 = 100 \mu\text{M}$, 358 kHz, 10 W, 0.605 L, 15 °C, $\text{pH}_{\text{initial}} \sim 5$). ▼: acoustic source remains on after $t=0$; ---: acoustic field is removed at $t=0$.

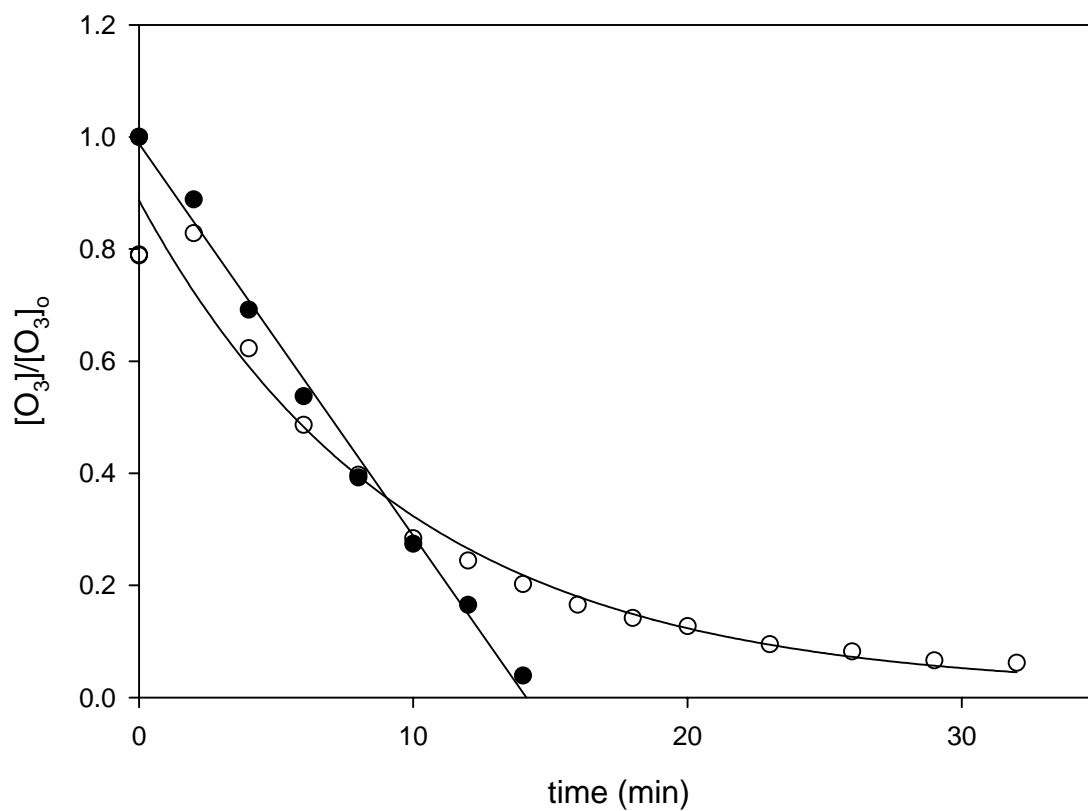


Figure 10: Ozone decay in ultrapure water. Ozone solution is pre-sonicated for 1 hour prior to $t=0$. The acoustic field remains on after $t=0$. ($[O_3]_0 = 100 \mu\text{M}$, 358 kHz, 10 W, 0.605 L, 15 °C). o: in neat water ($\text{pH}_{\text{initial}} \sim 5$); •: $[\text{H}_2\text{C}_2\text{O}_4]_0 = 0.9 \text{ mM}$ added at $t=0$ ($\text{pH}_{\text{initial}} \sim 3$)

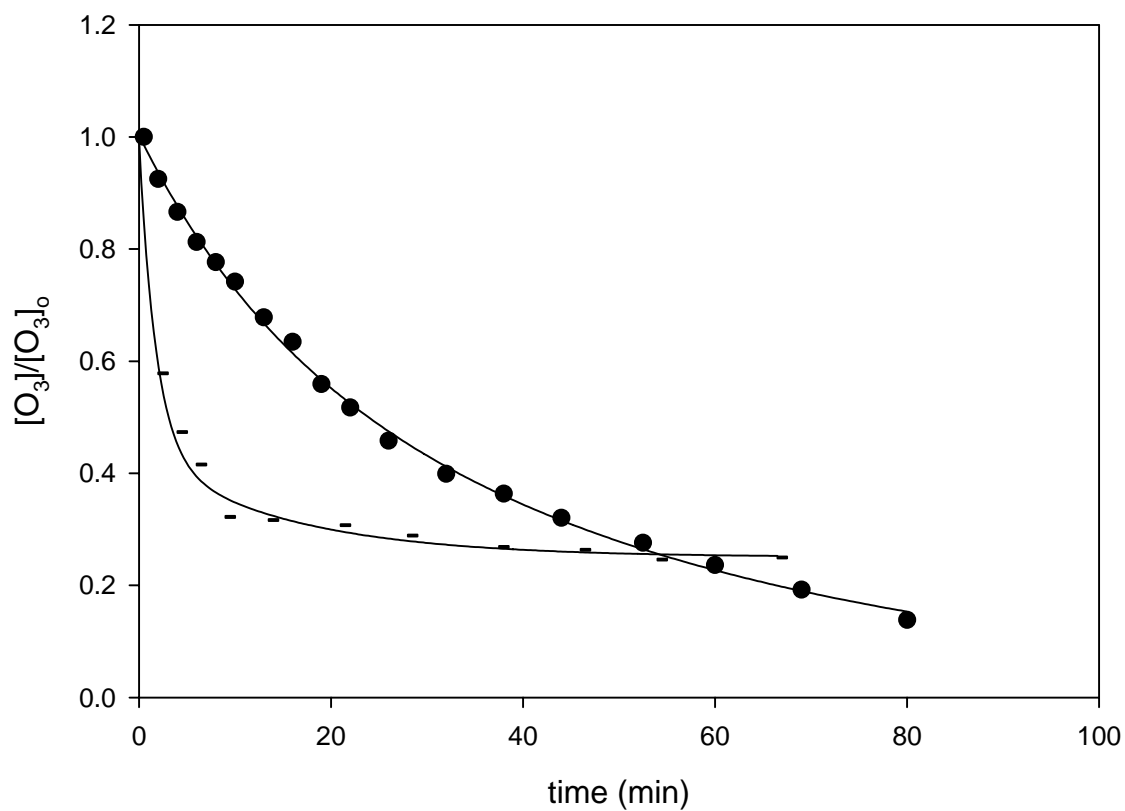


Figure 11: Ozone decay in ultrapure water. Ozone solution is pre-sonicated for 1 hour prior to $t=0$. The acoustic field is turned off after $t=0$. ($[O_3]_0 = 100 \mu\text{M}$, 358 kHz, 10 W, 0.605 L, 15 °C). ◻: in neat water ($\text{pH}_{\text{initial}} \sim 5$); ●: $[\text{H}_2\text{C}_2\text{O}_4]_0 = 0.9 \text{ mM}$ added at $t=0$ ($\text{pH}_{\text{initial}} \sim 3$).

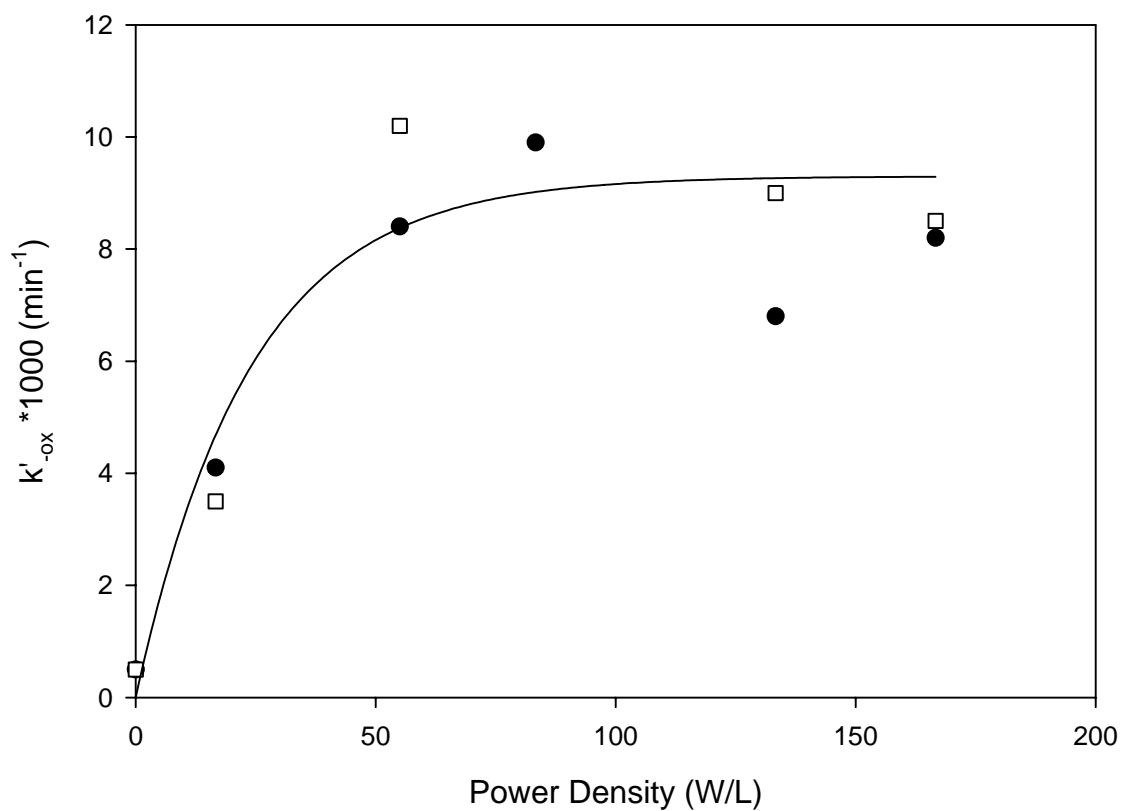


Figure 12: Normalized pseudo zero-order degradation rate constants of $[\text{H}_2\text{C}_2\text{O}_4]_t$ with ozone and ultrasound as a function of ultrasonic acoustic power. □: ultrasound pre-equilibrated with ozone 1 hour prior to the addition of oxalic acid; ●: ultrasound added simultaneously with the addition of oxalic acid. ($[\text{O}_3]_{ss} = 150 \mu\text{M}$, 358 kHz, $[\text{C}_2\text{H}_4\text{O}_4]_0 = 0.9 \text{ mM}$, 0.605 L, 15 °C, pH ~ 3)

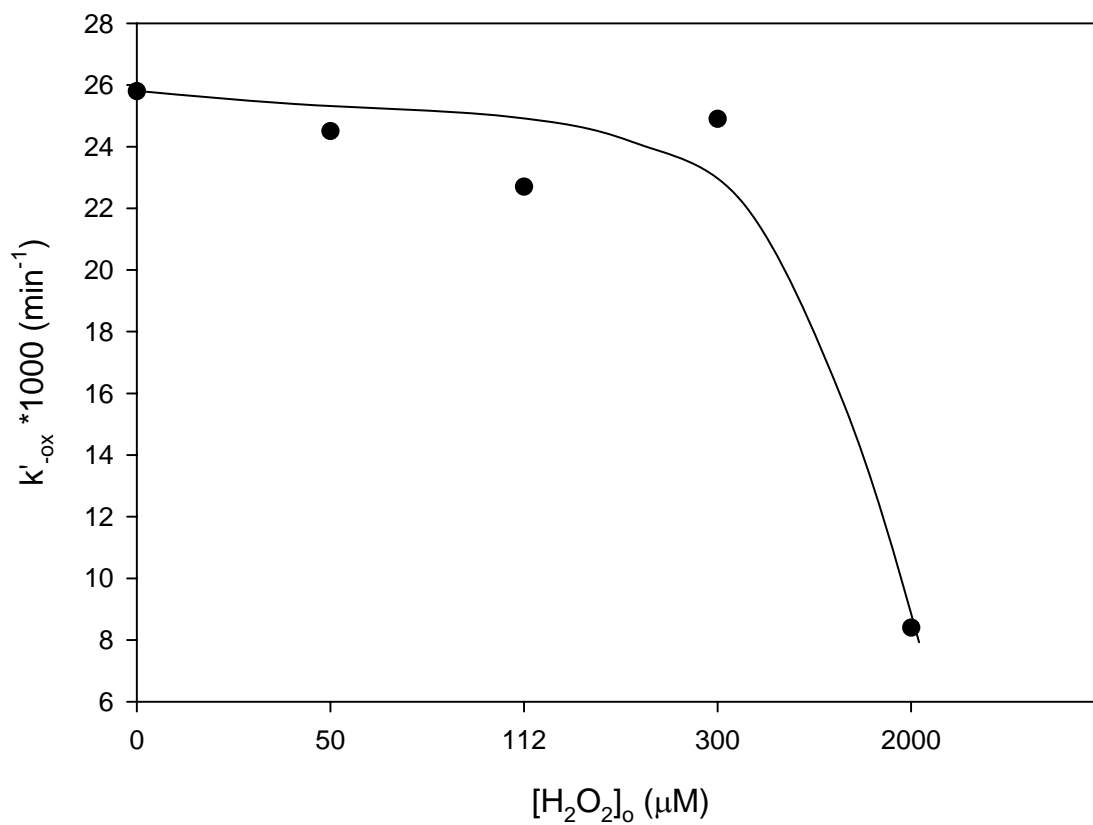


Figure 13: Normalized pseudo zero-order degradation rate constants of $[\text{H}_2\text{C}_2\text{O}_4]_t$ with ozone, ultrasound, and H_2O_2 . ($[\text{O}_3]_{\text{ss}} = 300 \mu\text{M}$, 358 kHz, 100 W, $[\text{C}_2\text{H}_4\text{O}_4]_0 = 0.9 \text{ mM}$, 0.605 L, 15 °C, pH ~ 3)

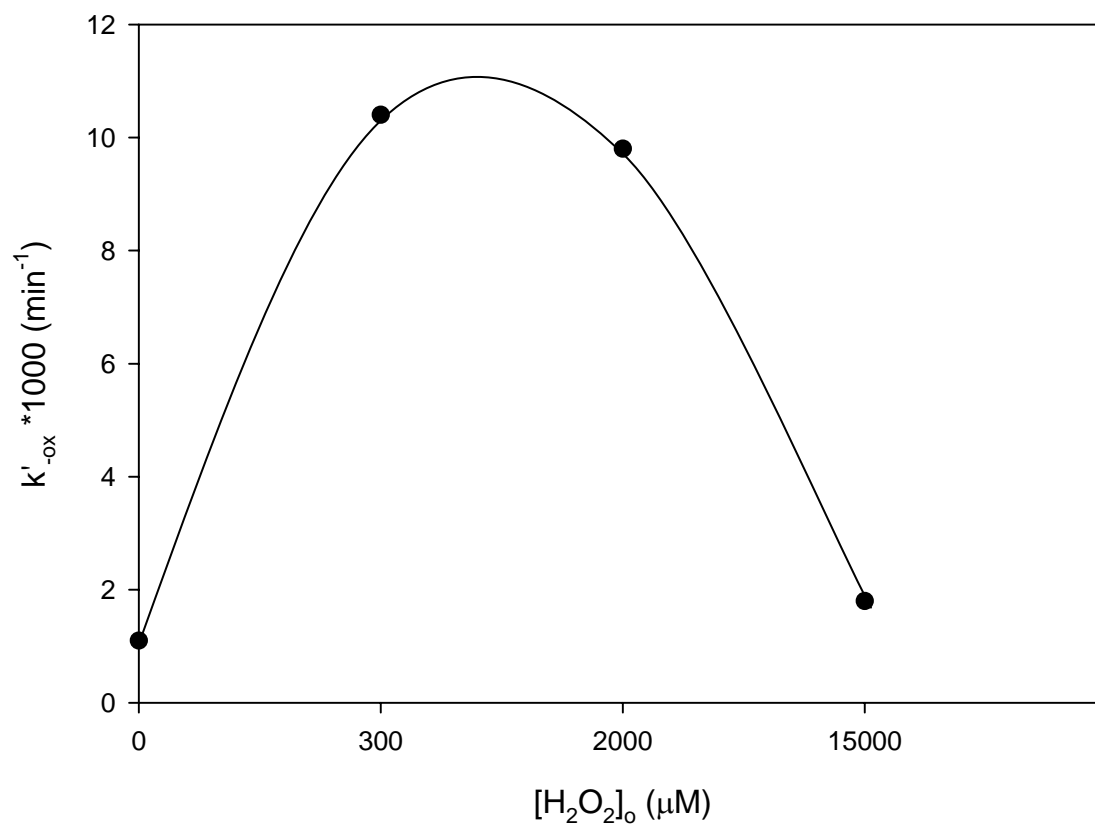


Figure 14: Normalized pseudo zero-order degradation rate constants of $[\text{H}_2\text{C}_2\text{O}_4]_t$ with ozone and H_2O_2 ($[\text{O}_3]_{\text{ss}} = 350 \mu\text{M}$, $[\text{C}_2\text{H}_4\text{O}_4]_o = 0.9 \text{ mM}$, 0.605 L, 15 °C, pH ~ 3)